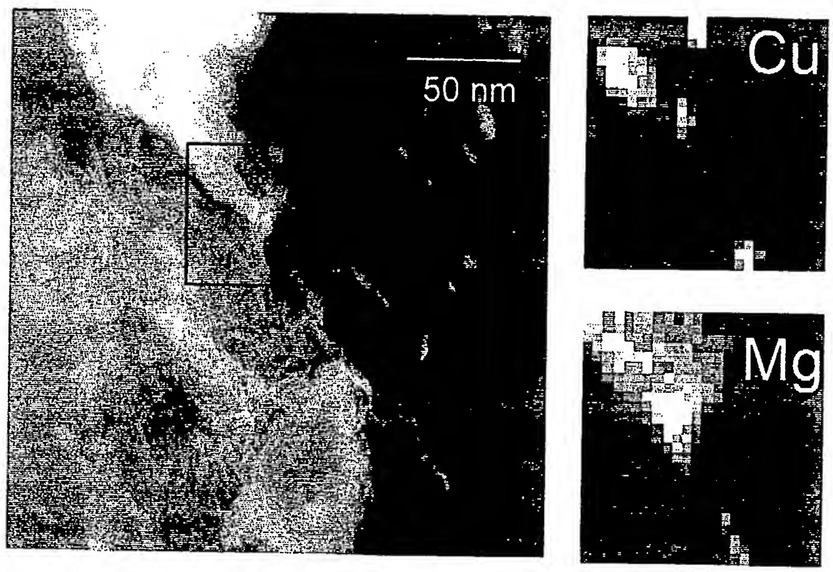

Figure 1 : Composition map of 5083+Cu demonstrates some descrete A-Mg-Cu particles at grain boundary, but Mg-rich β-phase still present.

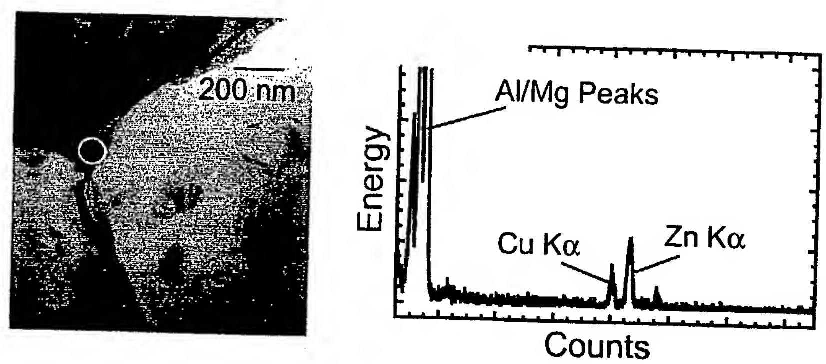

Figure 2 : EDS spectra of grain boundary phase in Zn+Cu-containing sample demonstrates observable levels of copper and zinc.

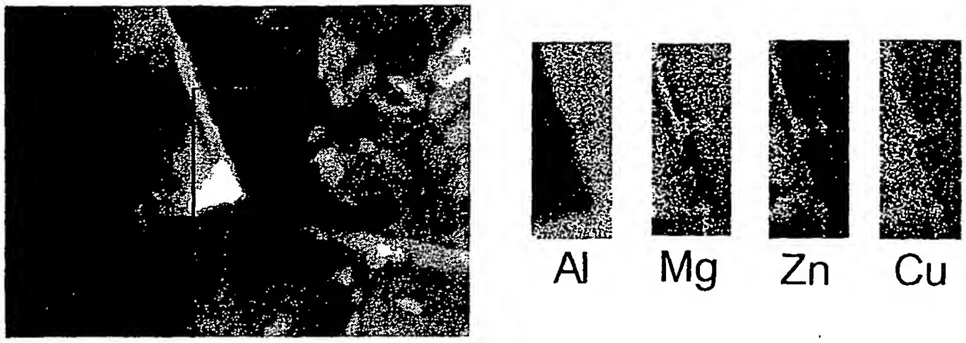

Figure 3 : Digital image of the grain boundary phases and associated composition maps of selected grain boundary area. EMiSPEC maps show relative levels of selected elements; brighter areas indicate higher concentration. Note the presence of copper in addition to the expected levels of magnesium and zinc

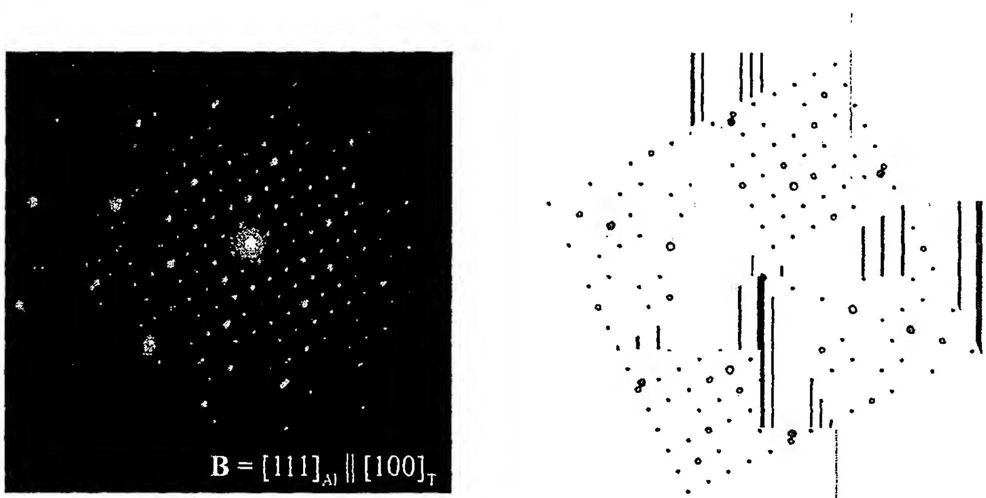

(a) (b)

Figure 4 : Diffraction pattern (a) of α-aluminum matrix and Al-Mg-Zn-Cu precipitate. The simulation (b), based on an $Mg_{32}(Al,Zn)_{49}$ precipitate in aluminum, agrees well with the observed pattern.

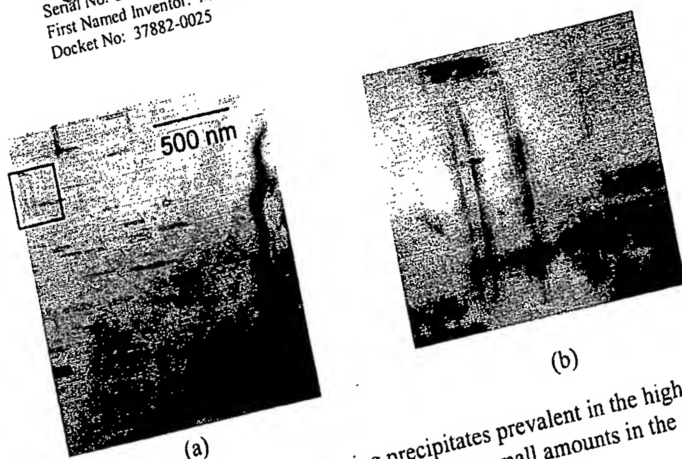

Figure 5 : Needle-shaped Cu-containing precipitates prevalent in the high-copper sample (inset (b) shows a close-up view); present in small amounts in the medium-copper sample and absent in the low-copper sample.

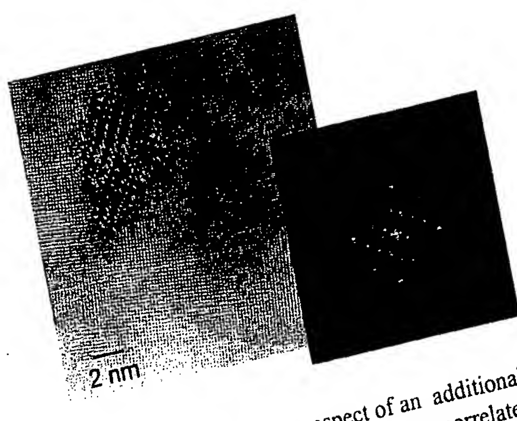

Figure 6 : High-resolution TEM image of one aspect of an additional phase precipitate. Associated Fourier transform (inset) of CCD image correlates very well with S-phase published work.

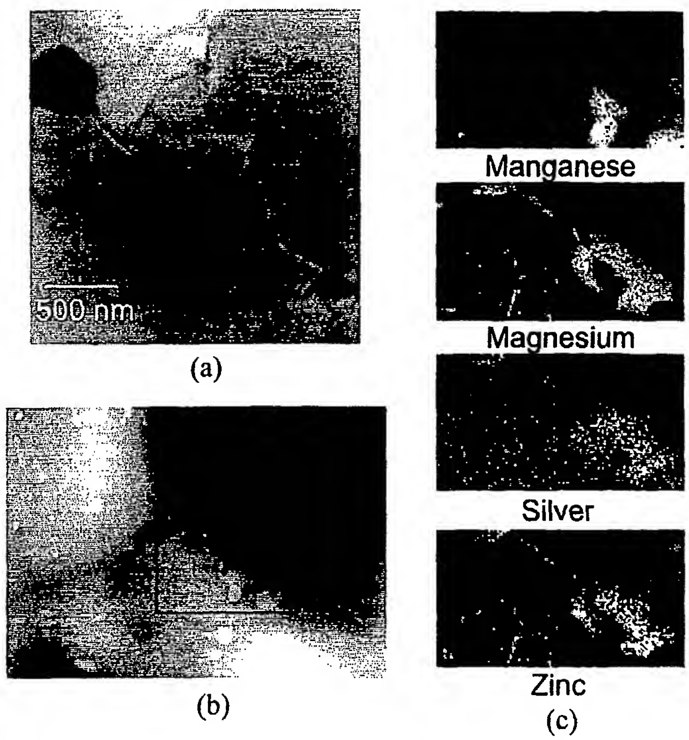

Figure 7 : 5083 + Zn + medium silver . Micrograph (a) and STEM image (b) demonstrate the grain boundary phase, while the presncepresence of silver, along with Mg and Zn, is clear from the composition maps (c).

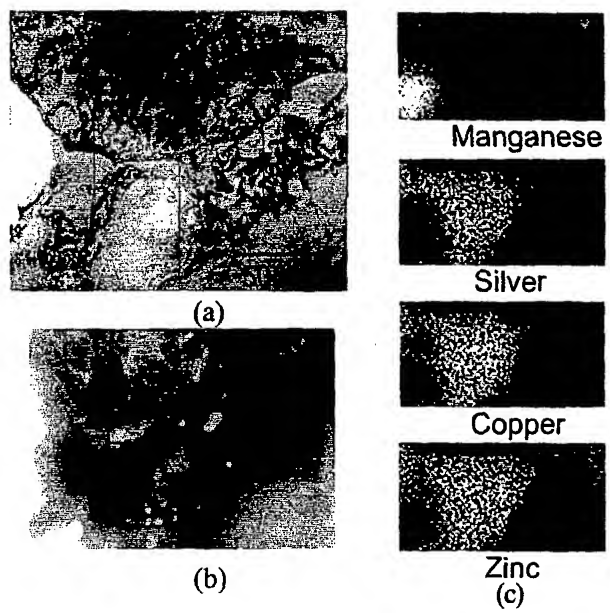

Figure 8 : 5083 + Zn + high copper *and* silver. Micrograph (a) and STEM image (b) demonstrate the grain boundary phase. Composition maps (c) show that a 5-component phase with both copper AND silver is present.

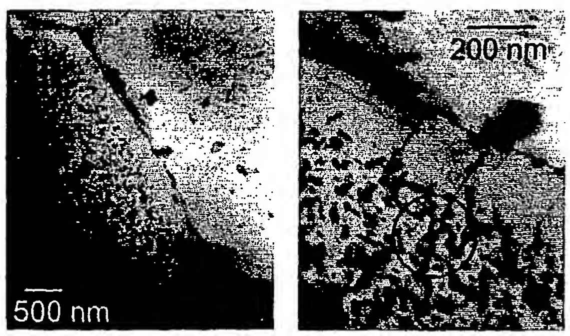

(a) (b)

Figure 9 : The high density of precipitates in the grain interior is present even in the alloys containing relatively low additions of Ag. The presence of a distinct precipitate-free zone is also demonstrated.

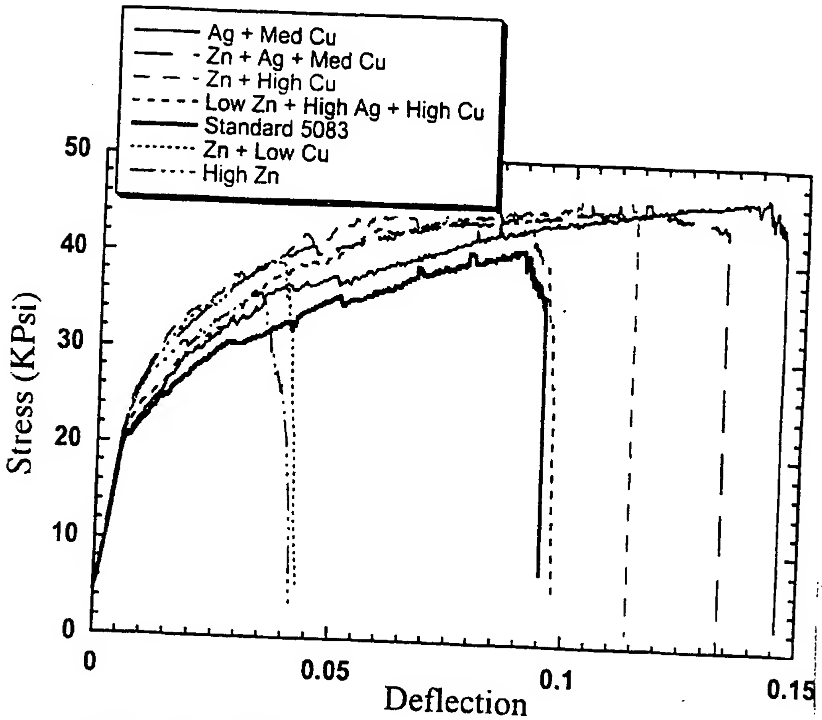

Figure 10 : SSRT results of modified alloys vs. standard 5083.

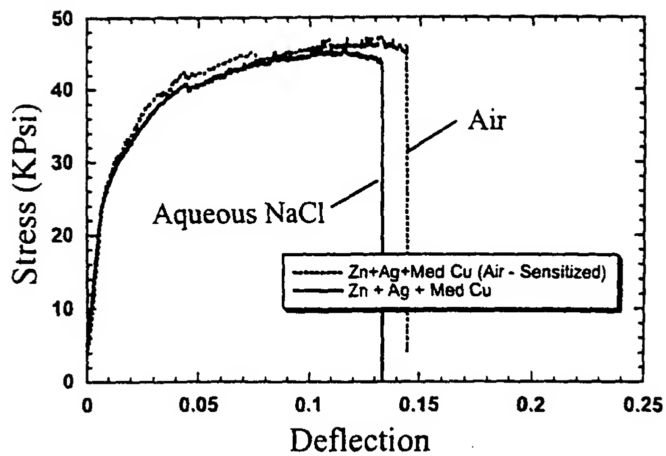

Figure 11 : CERT result for modified alloy in dry air vs. NaCl environment. The modified alloy has less initial ductility than standard 5083, but more of this ductility is retained with respect to SCC.

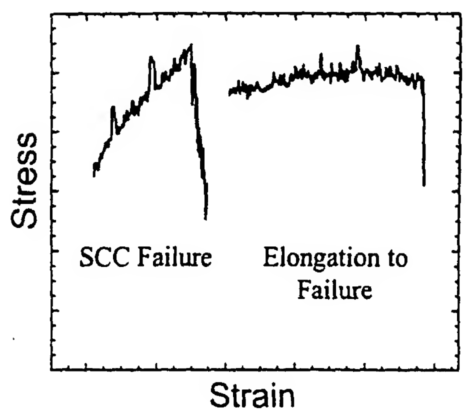

Figure 12 : Characteristic shapes of failure regions of tensile samples. SCC failure demonstrates a stepped series of stress drops rather than the gentle downward curve of engineering stress.

Title: 500[illegible]es Alloys With Improved Corrosion Properties and Meth[illegible] for Their Manufacture and Use
Serial No: Unassigned
First Named Inventor: Mark C. Carroll
Docket No: 37882-0025

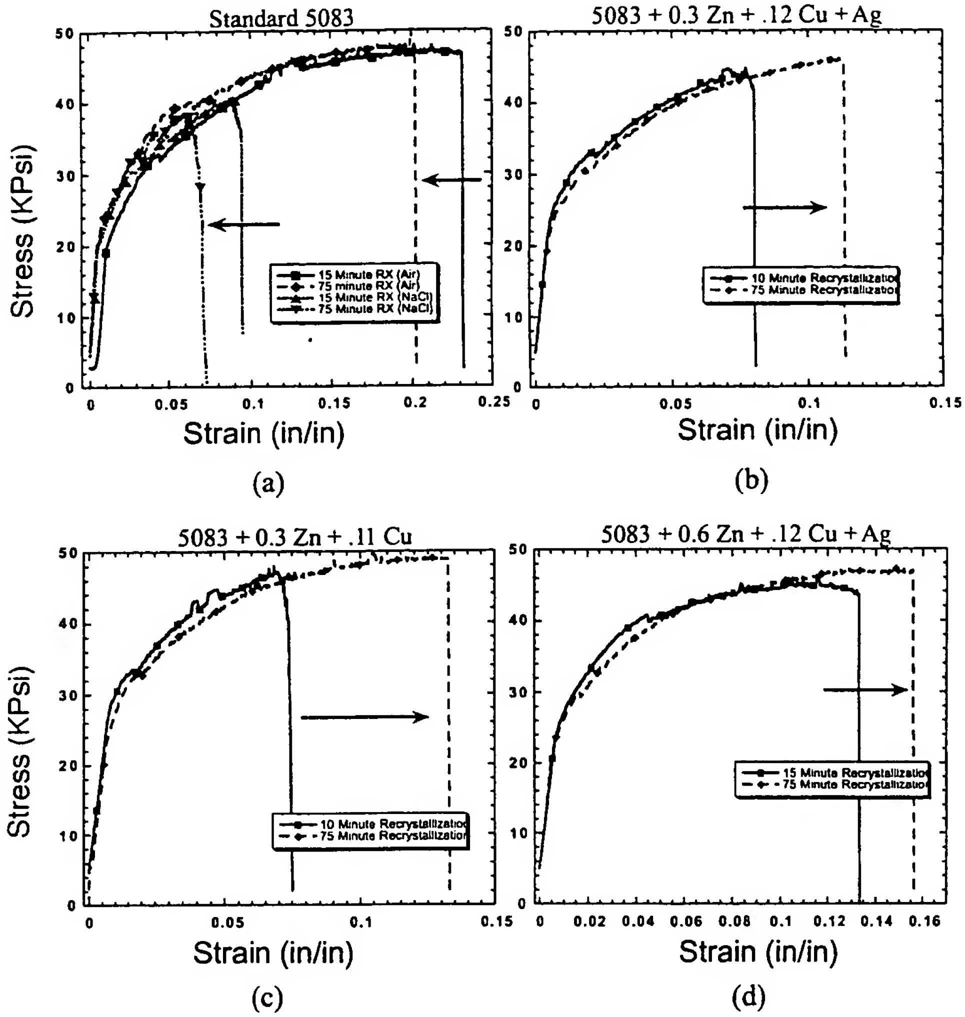

Figure 13 : Increasing the recrystallization treatment from 10-15 minutes to 75 minutes decreases the ductility of 5083 both in air and in aqueous NaCl (a), but increases ductility (SCC resistance) in modified alloys (b-d).

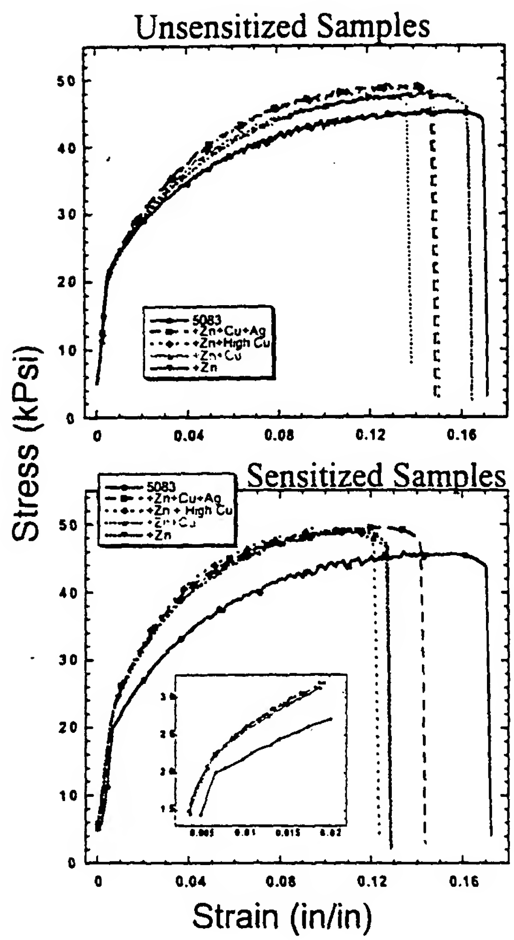

Figure 14 : Stress/strain curves for sensitized vs. unsensitized alloys pulled in air at 10^{-3}/second. Inset shows detail of yield point and associated increase in yield strength for modified alloys.

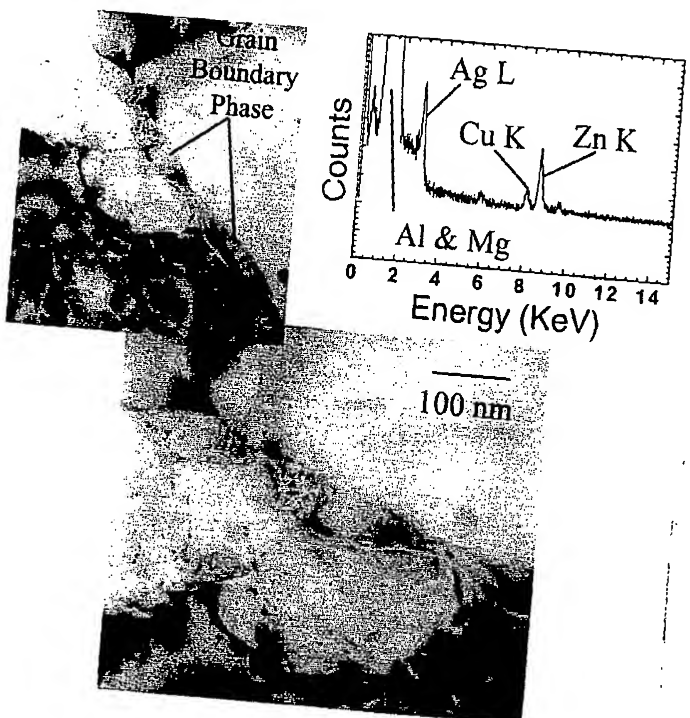

Figure 15 : Fine-probe EDS reveals the presence of Zn, Cu and Ag in the grain boundary region even at the reduced Zn level.

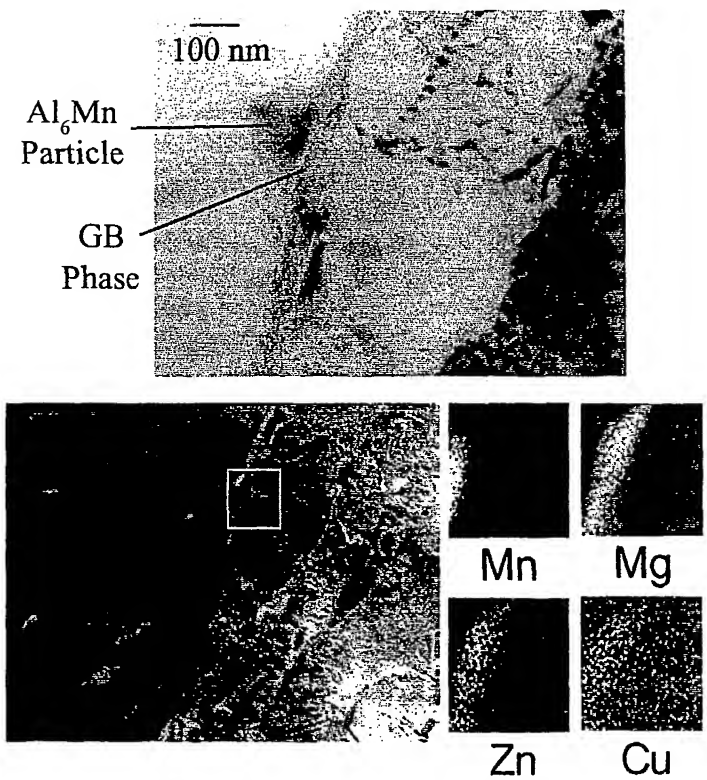

Figure 16 : Composition map of reduced-Zn sample; the grain boundary phase is in the Al_6Mn/grain boundary interface.

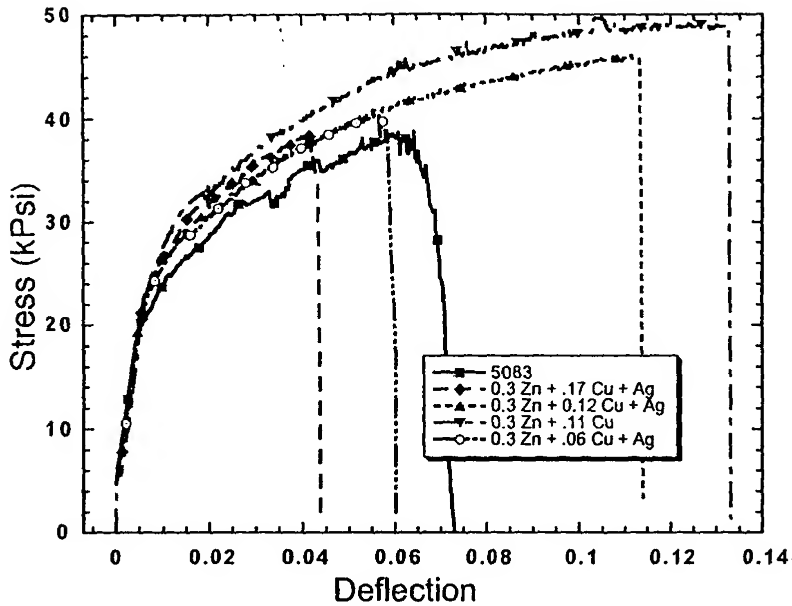

Figure 17 : CERT (aqueous NaCl) results of modified alloys with Zn level

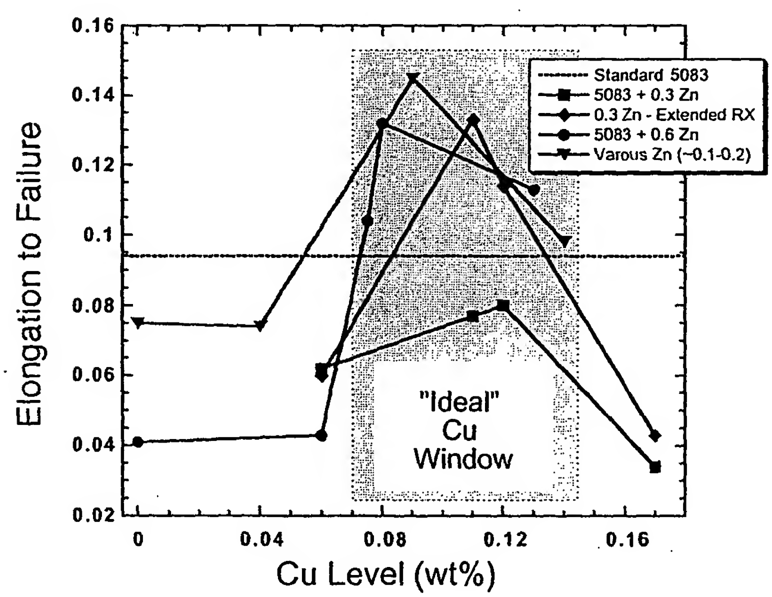

Figure 18 : An apparent optimum, or ideal , copper window exists with respect to SCC failure for low level additions in Zn-modified 5083 alloys.

Al-Mg-Zn-Cu precipitates

SEM micrographs obtained in Back Scattered Electron (BSE) mode

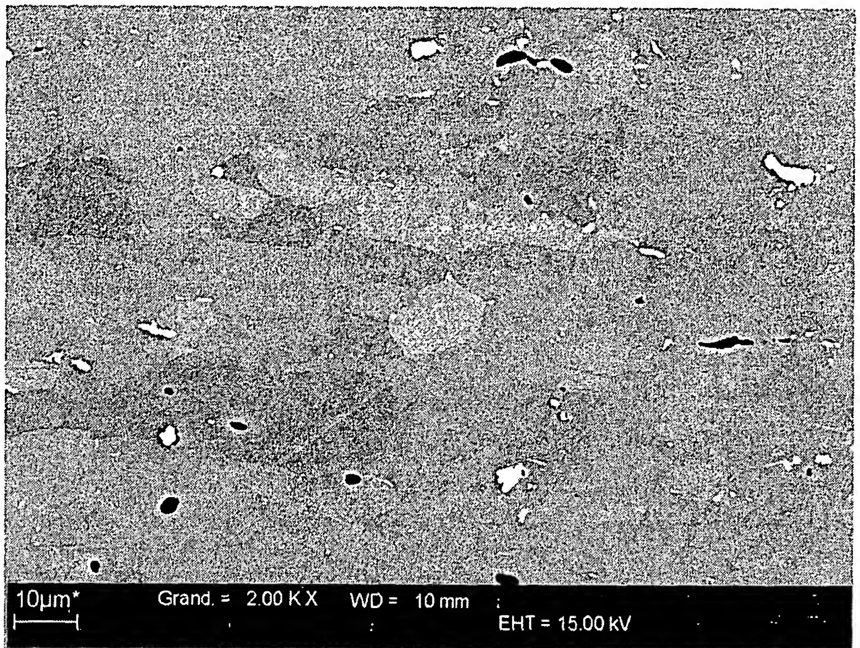

Fig 19 a)

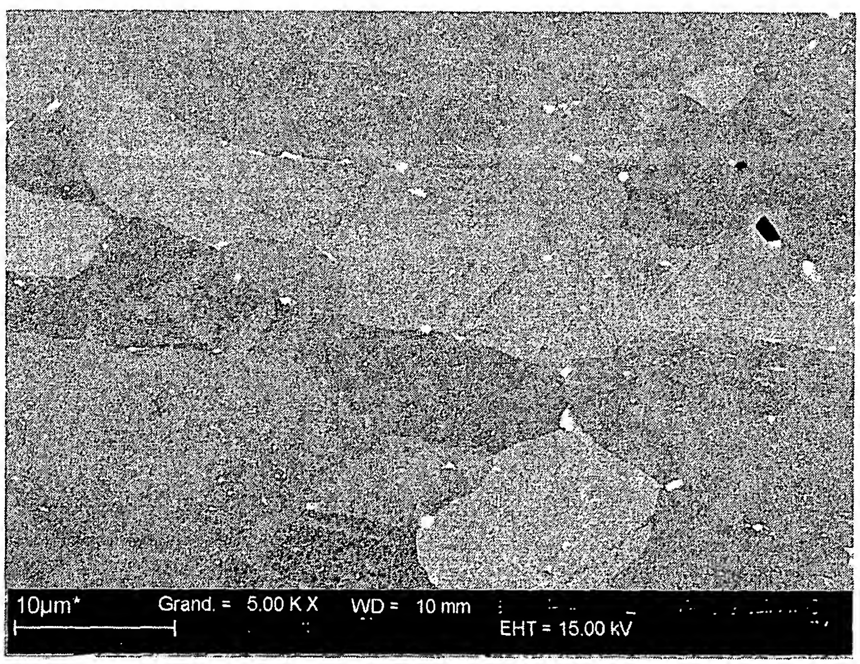

Fig. 19b

Desenstization of 5xxx alloys to intergranular corrosion

Search for Al-Mg-Zn-Cu precipitates :

SEM micrographs obtained in Back Scattered Electron (BSE) mode

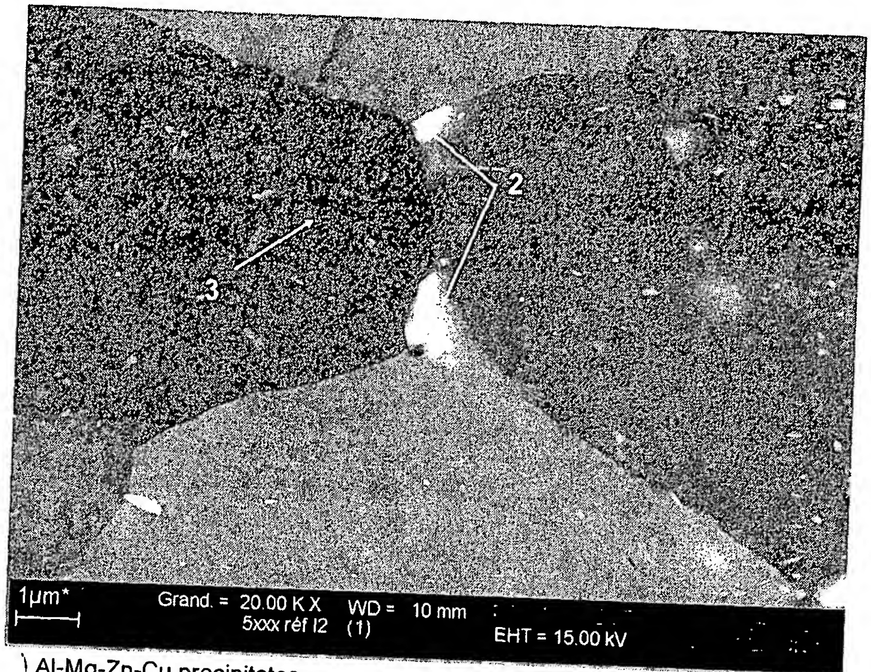

1 Al-Mg-Zn-Cu precipitates
2 Al-Mg-Zn-Cu
3 Al-Mg (matrix of 5xxx alloy)

Fig. 20

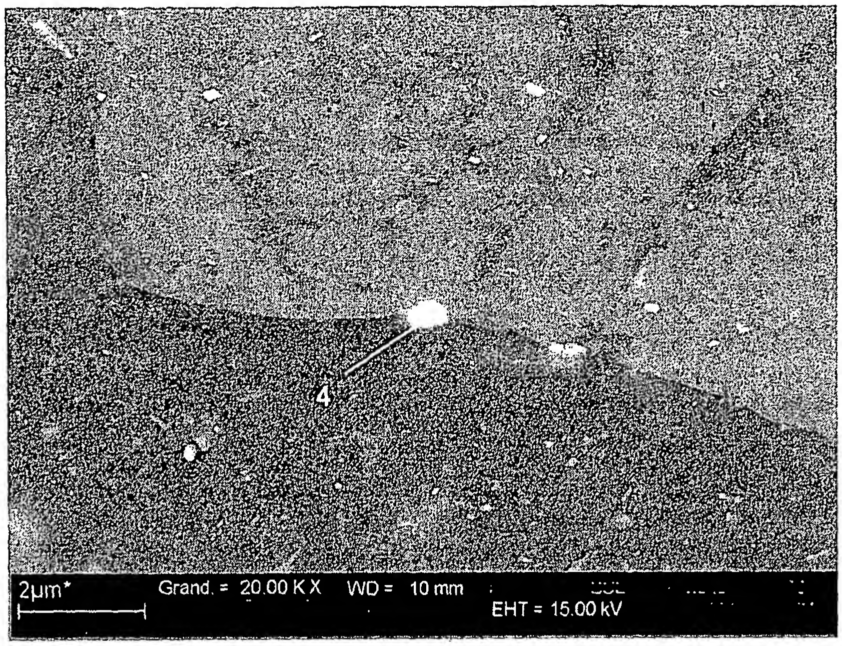

Précipité Al-Mg-Zn-Cu Al-Zn-Mg-Cu precipitate
4 Al-Mg-Cu-Zn)

Fig. 21

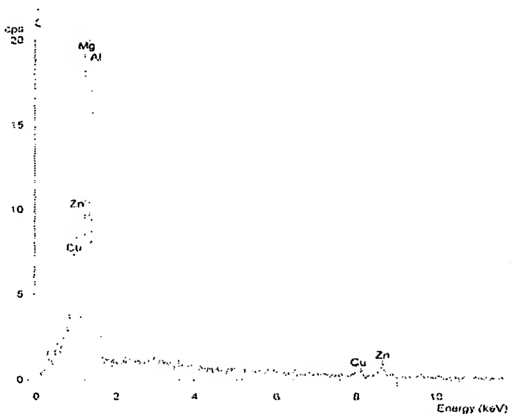

a) Spectre EDX 2 Al-Mg-Zn-Cu

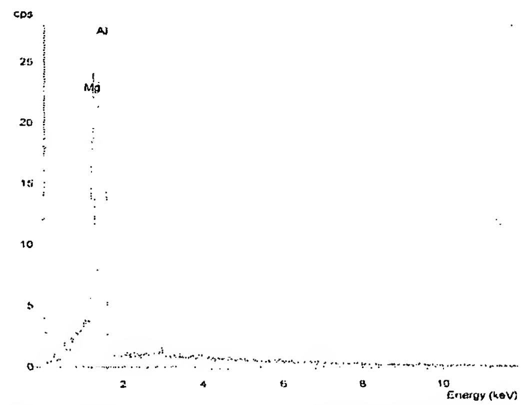

b) Spectre EDX 3 Al-Mg (matrice 5xxx)

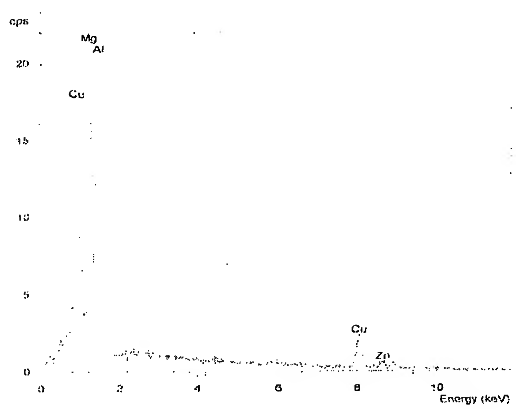

c) Spectre EDX 4 Al-Mg-Cu-Zn

Fig. 22a
22b
22c